Transactions, SMiRT-25
Charlotte, NC, USA, August 4-9, 2019
Division IV

Source Modelling for Reproducing of Strong Ground Motions and Permanent Displacements Very Close to the Fault Trace of the 2016 Kumamoto, Japan, Earthquake

Atsuko Oana[1], Kazuo Dan[2], Shinya Ikutama[3], Takeshi Kawasato[4], Masahiro Nosho[5], and Haruhiko Torita[6]

[1] Researcher, Ohsaki Research Institute, Inc., Tokyo, Japan (a.oana@ohsaki.co.jp)
[2] Research fellow, Ohsaki Research Institute, Inc., Tokyo, Japan
[3] Group Manager, Projects Development Dep., The Japan Atomic Power Company, Tokyo, Japan
[4] Manager, Projects Development Dep., The Japan Atomic Power Company, Tokyo, Japan
[5] Nuclear Projects Div., Shimizu Corporation, Tokyo, Japan
[6] Deputy director, Ohsaki Research Institute, Inc., Tokyo, Japan

ABSTRACT

The fault breakings appeared on the ground surface in the 2016 Kumamoto, Japan, earthquake (Mw7.1). The strong ground motions and permanent displacements were observed at stations very close to the fault trace during this earthquake. In this paper, we designated the fault rupture model of the 2016 Kumamoto earthquake which consists of the deep fault rupture model and the shallow fault rupture model, referring to Ikutama et al. (2018). Here, the upper depth of the deep fault rupture model was corresponded to the upper depth of the seismogenic layer based on the velocity structure model. It was shown that strong ground motions and permanent displacements of the simulation results using the fault rupture model reproduced well those of the observed records obtained in the area very close to the fault trace of the 2016 Kumamoto earthquake. It was also found that the ground motion generated by the shallow fault rupture greatly contributes to the characteristic velocity pulses and permanent displacements at Nishihara station, 0.7 km from the fault trace.

INTRODUCTION

The Recipe for strong ground motion prediction (Headquarters for Earthquake Research Promotion, 2016) is already available in Japan as a method for carrying out strong ground motion assessments, but simulating permanent displacements is not one of its objectives, and it gives no indication regarding modelling faults shallower than the top of the seismic fault (deep fault located within the seismogenic layer). In order to solve that problem, Ikutama et al. (2018) proposed a method of modelling that takes the entire ruptured fault from the ground surface to the seismic fault into account for evaluating strong ground motions and permanent displacements at sites very close to the fault trace.

In this paper, first, we reviewed the fault modelling method by Ikutama et al. (2018). Next, the method was applied to the 2016 Kumamoto earthquake (Mw7.1), and the fault rupture model of the 2016 Kumamoto earthquake is designated, consisting of the deep fault rupture model (from the top to the bottom of the seismic fault) and the shallow fault rupture model (from the ground surface to the top of the seismic fault) in Ikutama et al. (2018). At this time, the upper depth of the deep fault rupture model was corresponded to the upper depth of the seismogenic layer based on the velocity structure model. Finally, the fault rupture model was validated by the simulation of observed records obtained in the area very close to the fault trace of the 2016 Kumamoto earthquake.

FAULT MODELLING

Method for modelling the deep fault and the shallow fault

In this section, the fault modelling method by Ikutama et al. (2018) was explained briefly.

In order to evaluate strong ground motions and permanent displacements at sites very close to the fault trace, Ikutama et al. (2018) proposed the fault model as shown in Figure 1. This model consists of the deep fault from the top to the bottom of the seismic fault (the fault covered by the Recipe for strong ground motion prediction), and the shallow fault model that covers the area above that (from the ground surface to the top of the seismic fault).

For the deep fault, parameters are set in accordance with the Recipe for strong ground motion prediction published by Headquarters for Earthquake Research Promotion (2016) as shown in Figure 2 (a).

The shallow fault is an area that is not modelled by the Recipe for strong ground motion prediction. Because it is considered that the rupture in this area occurs passively in association with the deep fault slip, and that there is no autonomous rupture, and therefore stress drop is assumed to be zero. Ikutama et al. (2018) designated the shallow fault directly above the asperity as the large-slip area, and the shallow fault directly above the background as the small-slip area, as shown in Figure 2 (b). As methods of determining the slip on the large-slip area D_{large}, Ikutama et al. (2018) recommended the following three options. The first is using a unit displacement per one earthquake in cases when it has been obtained from geological surveys, the second is using the empirical relationship by Matsushima *et al.* (2010), describing a relationship between the maximum slip at the ground surface and the averaged slip on the seismic fault, and the third is using the empirical relationship by Matsuda (1975), describing a relationship between the slip and the active fault length. The slip on the small-slip area D_{small} is taken to be the value of the slip for the large-slip area D_{large} adjusted by the ratio of the asperity slip D_a to the background slip D_b as follows:

$$D_{small} = D_{large} \cdot \frac{D_b}{D_a} . \tag{1}$$

The seismic moment increase by adding the shallow fault will be equivalent to about 10% of the seismic moment of the deep fault under assumption that the modulus of rigidity of the shallow fault is half that of the deep fault.

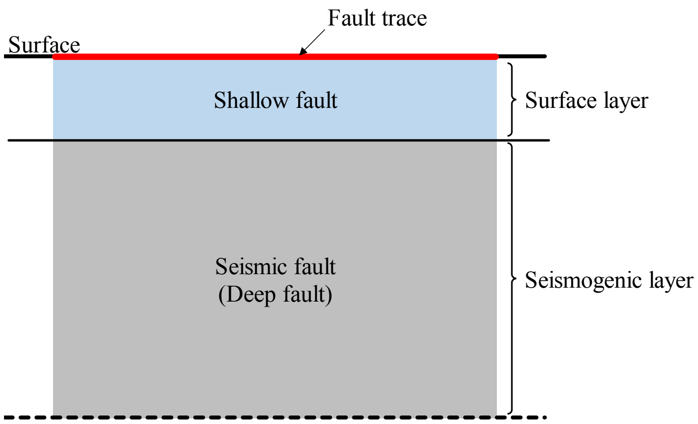

Figure 1. Outline of the fault model (Ikutama et al., 2018).

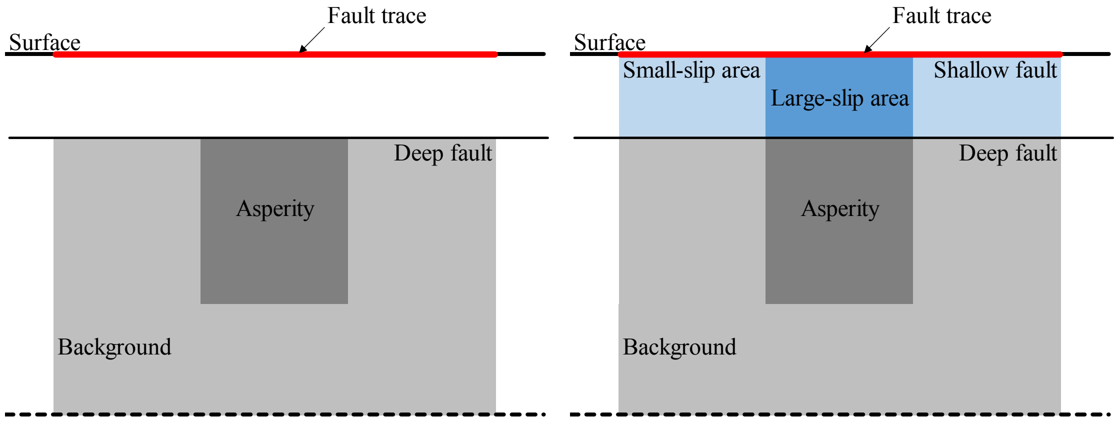

(a) Deep fault (b) Deep and shallow faults

Figure 2. Models for deep and shallow faults.

Fault rupture model of mainshock of the 2016 Kumamoto earthquake

Ikutama et al. (2018) proposed a fault rupture model (deep and shallow fault models) for the 2016 Kumamoto earthquake based on the fault modelling method summarized in the previous section. The deep fault model was taken from the characterized source model (strong motion generation area model) by Oana et al. (2017). While the upper depth of the characterized source model by Oana et al. (2017) is 2 km, the upper depth of the seismogenic layer based on the velocity structure model is 3.283 km. However, these two values should be the same originally. In order to eliminate the difference between them, the upper depth of the deep fault model by Ikutama et al. (2018) was revised from 2 km to 3.283 km. The stress drops on the asperities were also adjusted by trial and error so that the observed short-period (about < 5 seconds) strong ground motions at stations very close to the fault trace were reproduced well. The deep fault width was assumed to be 16.56 km so as to correspond to the small earthquake distribution and to also correspond to the lower depth of the seismic fault model by Ikutama et al. (2018). The fault length and the slip on the asperities are the same as those in Ikutama et al. (2018). The slip on the background area was assigned from the seismic moment obtained by subtracting the sum of the seismic moment of the asperities from the F-net estimate (4.42×10^{19} Nm). The effective stress on the background area was assumed to be 20 % of the average stress drop on the asperities, taking into account the approximate ratio of the effective stress on the background area to the stress drop on the asperity, which is obtained from the asperity model based on the Recipe.

We assigned the large-slip area directly above asperity 1. According to National Institute of Advanced Industrial Science and Technology (AIST) (2016), the ground surface displacement was measured about 2 m (total amplitude). On the other hand, the results of urgent GNSS observations by the Geospatial Information Authority of Japan (GSI) (Ueshiba et al., 2016) demonstrated that there had been subsidence of about 2 m (half amplitude) in the Nishihara village, and a permanent displacement of 2 m (half amplitude) can be seen in the displacement waveform observed at the Nishihara station (Iwata, 2016). In some previous numerical analyses for the 2016 Kumamoto earthquake (e.g. Irikura and Kurahashi(2017), Matsumoto et al. (2017), Nosho et al. (2018)), they showed that the simulated permanent displacement at the Nishihara village by the model in which the slip on the top surface layer (< depth of 300 m) of large-slip area D_{large} is 2 m and the slip on the surface layer (depth of 300 m to 2 km or 3 km) of large-slip area D_{large} is 4 m was almost the same as that of the model which the whole large-slip area D_{large} is 4 m. The difference between the surface displacement of the survey result and the permanent displacement obtained from the observed displacement waveform was interpreted through their studies. According to their models, we set the D_{large} to 4 m (as total amplitude). The slip on the small-slip area D_{small} was determined by equation (1) in the previous section.

Rupture propagation mode was taken to be circular in each segment, as in Oana et al. (2017). The rupture velocity was set to be 2.7 km/s on asperity 2, and to 3.0 km/s elsewhere. The fault rupture model is shown in Figure 3. The map of the fault rupture model and the observation stations are shown in Figure 4.

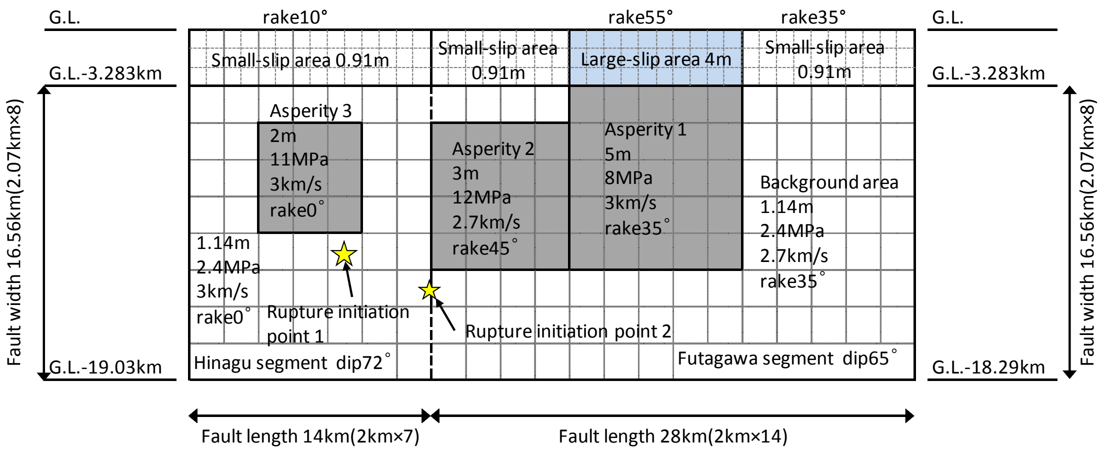

The value in the figure mean slip[m], stress drop or effective stress[MPa], and rupture velocity[km/s].

Figure 3. Fault rupture model of the mainshock of the 2016 Kumamoto, Japan, earthquake.

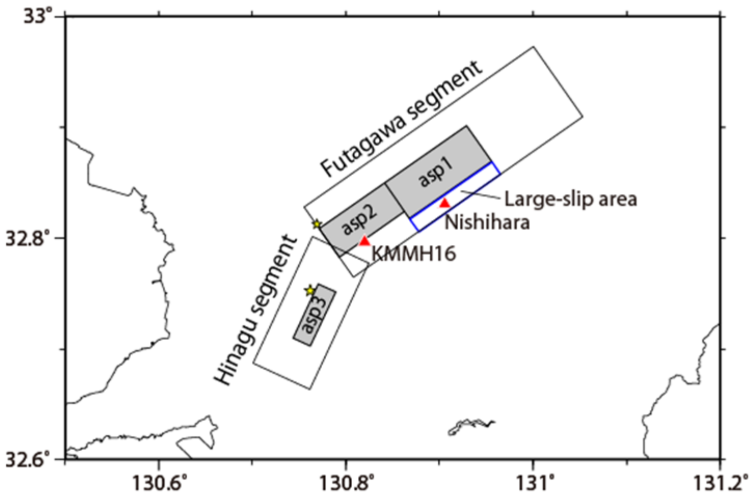

Figure 4. Map of the fault rupture model and the observation stations.

STRONG MOTION EVALUATION METHOD

The strong ground motion evaluation for the deep fault was carried out by the hybrid synthesis method incorporating the stochastic Green's function method (for short-period ground motions) and the wavenumber integration technique (for long-period ground motions) by Hisada and Bielak (2003). The strong ground motion evaluation for the shallow fault was carried out by the wavenumber integration technique because we assumed that the effects of the shallow fault appear in the long period range. A time lag between a simulation result by the stochastic Green's function method and that by the wavenumber integration technique was taken to be the difference of *S*-wave onset time by the ray theory. The hybrid period of the matching filter in the frequency domain was set to be 1 second. The low-pass filter for the simulation results of the shallow fault was the same as that for the simulation results of the deep fault by the wavenumber integration technique.

We used the synthesis method by Dan et al. (1989) for the stochastic Green's function method. The cutoff frequency f_{max} was assumed to be 4 Hz as in Oana et al. (2017). The path Q-value was 62 $f^{0.87}$ (constant value below 1 Hz) taken from Satoh (2016). The transition frequency of radiation pattern was set to be 3 to 6 Hz (Satoh, 2002). That is, a radiation coefficient was set to be the theoretical value (Aki and Richards, 1980) below 3 Hz, and the value for the omnidirectional average (Boore and Boatwright, 1984) over 6 Hz. The stochastic Green's functions were generated using the stochastic amplitude model and the envelope function model (Boore, 1983) which was especially developed for the area close to the fault. Then, the waves that had bell-shape forms were selected based on Kagawa (2004).

In the calculation by the wavenumber integration technique, we used a triangular function as a slip velocity time function, and obtained the rise time τ for the deep fault by Somerville et al. (1999) as follows:

$$\tau\,[\mathrm{s}] = 2.03 \times 10^{-9} \times (M_0\,[\mathrm{N \cdot m}] \times 10^7)^{1/3}\,. \qquad (2)$$

We also used a triangular function as a slip velocity time function for the shallow fault, and we assumed the maximum slip velocity on the large-slip area to be half of that on the asperity 1, and the maximum slip velocity on the small-slip area to be half of that on the background area, as Ikutama et al. (2018) did. The slip velocity time functions for the deep and shallow faults were shown in Figure 5.

The velocity structure model of Mashiki station (KMMH16) from the upper depth of the seismogenic layer (G.L.-3.283 km) to the engineering bedrock (G.L.-101 m) was assumed based on the boring data by K-NET and the Japan integrated velocity structure model (Koketsu et al., 2012), then that model was adjusted so that the dominant frequency of the model corresponded to that of the H/V spectral ratio of the small aftershock records. Figure 6 shows the adjusted velocity structure model. We assumed that the velocity structure model of Nishihara station was the same as that of Mashiki station. For both the observed records and simulation results, the strong ground motions were obtained on the engineering bedrock.

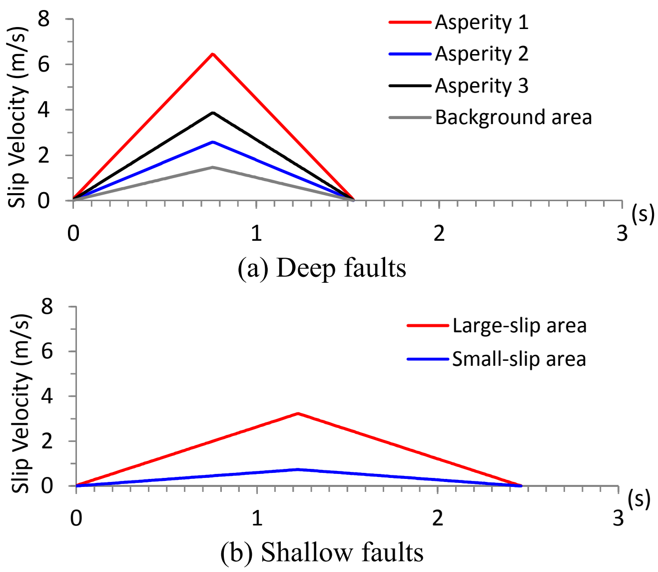

Figure 5. Slip velocity time functions on deep and shallow faults.

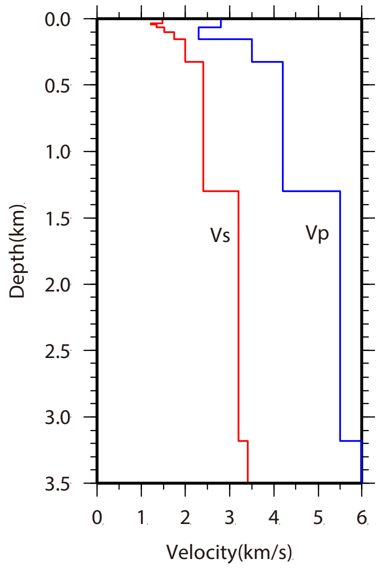

Figure 6. Velocity structure model at Mashiki station (KMMH16).

SIMULATION RESULTS

We compared the simulation results with the observed records at Mashiki and Nishihara stations. These two stations are close to the fault trace for the 2016 Kumamoto earthquake: Mashiki is 2 km from the trace and Nishihara is 0.7 km from the trace.

Figure 7 compares the velocity waveforms of the observed records with the simulation results. The simulation results by the whole fault reproduced the observed records well at both Mashiki and Nishihara stations. Figure 7(a) shows that the simulation results at Mashiki station by the deep fault alone are almost the same as those by the whole fault, thus it is clear that the strong ground motions generated by the deep fault are larger than those by the shallow fault. On the other hand, Figure 7(b) shows that the simulation results at Nishihara station by the deep fault alone are much smaller than those by the whole fault, and underestimate the observed records. Also, it seems that the strong ground motions generated by the shallow fault alone are dominant in the motions generated by the whole fault, and that the characteristic velocity pulses are generated by the shallow fault. It is considered that the difference between two stations regarding the contribution of the strong ground motions from the shallow fault is caused by the distance from the large-slip area to each site.

Figure 8 compares the displacement waveforms of the observed records with the simulation results. Figure 8(a) shows that while the simulation result of the EW component at Mashiki station by the whole fault underestimates the observed record, those of the NS and UD components agree with the observed records. It can be considered that the effect of shallow fault is small, and taking just the deep fault into account is sufficient for reproducing the observed records at Mashiki station. Figure 8(b) shows that the simulated permanent displacements of the EW and UD components by the deep fault alone underestimate the observed records, but if the shallow fault is also taken into account, the results of the NS, EW, and UD components agree pretty well with the observed records. It can be seen that the most of the permanent displacements at Nishihara station are determined by the shallow fault rupture. The risetime of the waveform (the time from the onset to reach the maximum displacement) was reproduced well at both stations, which indicates that the risetime of the slip velocity function is appropriate.

Figure 9 compares the simulated pseudo velocity response spectra (h=0.05) with the observed ones. For both Mashiki and Nishihara stations, they correspond to the observed spectra over broadband. Figure 9(a) shows that, for period range over 1 second, the simulation results by the deep fault alone are almost the same as those by the whole fault at Mashiki station, thus it is clear that the strong ground motions generated by the deep fault are larger than those by the shallow fault. The simulation results by the deep fault alone are much smaller than those by the whole fault for period range over 1 second at Nishihara station, and also underestimate the observed records, and it seems that the dominant period 2-4 s is derived from the ground motions generated by the shallow fault.

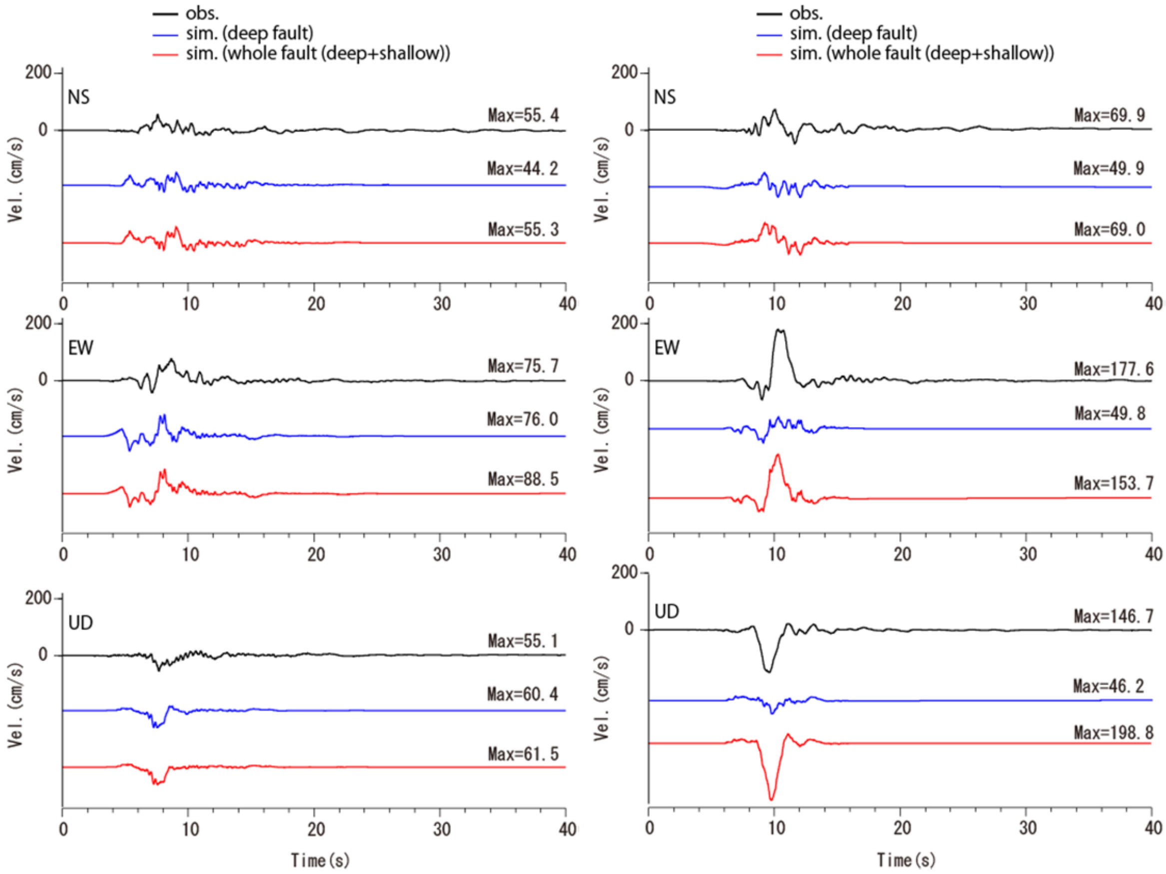

(a) Mashiki station (KMMH16) (b) Nishihara station

Figure 7. Comparison of the simulated velocity waveforms with the observed ones.

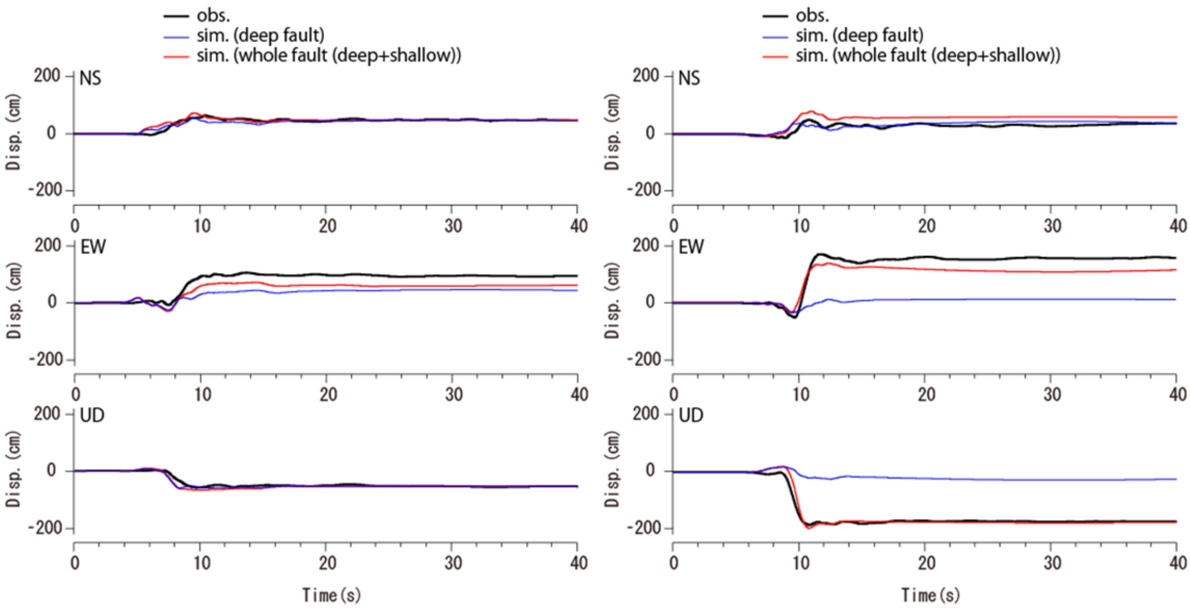

(a) Mashiki station (KMMH16) (b) Nishihara station

Figure 8. Comparison of the simulated displacement waveforms with the observed ones.

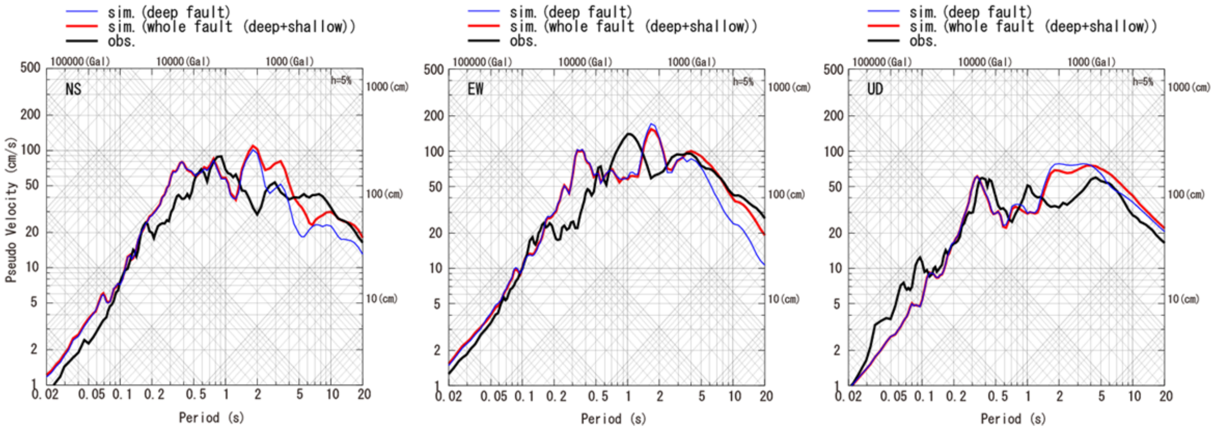

(a) Mashiki station (KMMH16)

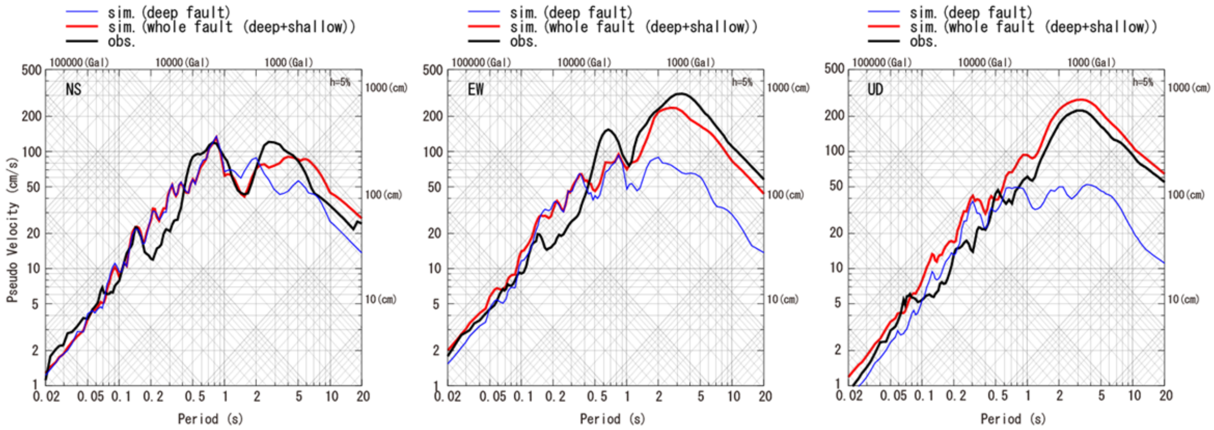

(b) Nishihara station

Figure 9. Comparison of the simulated pseudo velocity response spectra (h=0.05) with the observed ones.

CONCLUSIONS

We designated the fault rupture model of the 2016 Kumamoto earthquake which consists of the deep fault rupture model and the shallow fault rupture model as in Ikutama et al. (2018). Here, the upper depth of the deep fault rupture model by Ikutama et al. (2018) was revised from 2 km to 3.283 km in order to correspond to the upper depth of the seismogenic layer based on the velocity structure model. Using that fault rupture model, we tried to reproduce the observed records at Mashiki and Nishihara stations very close to the fault trace. As a result, the fault rupture model was validated by good reproductions of the strong ground motions and permanent displacements at both stations. It was found that the ground motion generated by the shallow fault rupture greatly contributes to the characteristic velocity pulses and permanent displacements at Nishihara station, 0.7 km from the fault trace.

ACKNOWLEDGEMENTS

We are grateful to the National Research Institute for Earth Science and Disaster Resilience, JMA and Kumamoto Prefecture for enabling us to use the observed records. We express our gratitude to Prof. Yoshiaki Hisada at Kogakuin University, Tokyo, for generously providing program for the wavenumber integration method on his website. We also express our gratitude to Mr. Meguru Sakai of Ohsaki Research Institute for his help in drawing the figure and calculating.

REFERENCES

Aki, K. and P.G. Richards(1980). "Quantitative Seismology," W.H.Freeman and Company, New York.

Boore, D. M.(1983). "Stochastic simulation of high-frequency ground motions based on seismological models of the radiated spectra," *Bulletin of the Seismological Society of America*, Vol. 73, No. 6, 1865-1894.

Boore, D. M. and J. Boatwright (1984). "Average body wave radiation coefficient," *Bulletin of the Seismological Society of America*, Vol.74, 1615-1621.

Dan, K., T. Watanabe, and T. Tanaka (1989). "A semi-empirical method to synthesize earthquake ground motions based on approximate far-field shear-wave displacement," *Journal of Structural and Construction Engineering* (Transactions of AIJ), No. 396, 27-36.

Headquarters for Earthquake Research Promotion (2016). "Strong ground motion prediction method for earthquakes with specified source faults ("Recipe")" (in Japanese).

Hisada, Y. and J. Bielak(2003). "A Theoretical method for Computing Near-Fault Ground Motions in Layered Half-Spaces Considering Static Offset Due to Surface Faulting, with a Physical Interpretation of Fling Step and Rupture Directivity," *Bulletin of the Seismological Society of America*, Vol.93, No.3, 1154-1168.

Ikutama, S., Kawasato, T., Kawakami, Y., Nosho, M., Oana, A., Dan, K., Torita, H. and Okada, Y. (2018). "Source modeling for prediction ground motions and permanent displacements very close to the fault trace," *Journal of Earthquake and Tsunami*, Vol.12, No.4, 1841005.

Irikura, K. and Kurahashi, S. (2017). "Extension of a characterized source model for long-period ground motion estimation near the fault –Verification by near-fault ground motion of the 2016 Kumamoto earthquake (Mw7.0)," *Proceedings of the 13th Annual Meeting of Japan Association for Earthquake Engineering*, P3-2 (in Japanese).

Iwata, T. (2016). "Kumamoto earthquake 3-month report. 2. Information about the earthquake: strong ground motions, source process, strong motion observations," *Symposium organized by Science Council of Japan* (in Japanese).

Kagawa, T. (2004). "Developing a stochastic Green's function method having more accuracy in long period range to be used in the hybrid method," *Journal of Japan Association for Earthquake Engineering*, Vol.4, No.2, 21-32 (in Japanese with English abstract).

Koketsu, K., Miyake, H. and Suzuki, H. (2012). "Japan integrated velocity structure model version 1," *Proceedings of the 15th World Conference on Earthquake Engineering*.

Matsuda, T. (1975). "Magnitude and recurrence interval of earthquakes from a fault," *Zisin*, 28(3), 269-283 (in Japanese with English abstract).

Matsumoto, Y., Miyakoshi, K., Irikura, K. and Takahama, T. (2017). "Characterized source model for estimating long-period (more than 2s-) ground motions including permanent displacement of the 2016 Kumamoto earthquake (Mj7.3)," *Japan Geoscience Union Meeting 2017*, S15-P02 (in Japanese).

Matsushima, S., Murotani, S., Azuma, T., Irikura, K. and Kitagawa, S. (2010). "Scaling relations of earthquakes on active mega-fault systems," *Geophysical Bulletin of Hokkaido University*, 73, 117-127 (in Japanese with English abstract).

National Institute of Advanced Industrial Science and Technology (AIST) (2016). "Surface ruptures emerging in association with the 2016 Kumamoto earthquake," Report 4 (May 13, 2016): Emergency Survey Report, AIST website (in Japanese).

Nosho, M., Ikutama, S., Sawairi, M., Oana, A., Dan, K. and Torita, H. (2018). "Source model for prediction of ground motions and permanent displacements close to the fault trace, Part 5: Simulation of the strong motion records from the mainshock of the 2016 Kumamoto earthquakes considering the slip on the fault trace," *Summaries of Technical Papers of Annual Meeting of Architectual Institute of Japan*, 759-760 (in Japanese).

Oana, A., Dan, K., Miyakoshi, J., Fujiwara, H., Morikawa, N. and Maeda, T. (2017). "Estimation of characterized source model of the mainshock in the 2016 Kumamoto earthquakes using the stochastic Green's function method," *Japan Geoscience Union Meeting 2017*, SCG70-P04.

Satoh, T. (2002). "Radiation pattern and fmax of the Tottori-ken Seibu earthquake and the aftershocks inferred from KiK-net strong motion records," *Journal of Structural and Construction Engineering* (Transactions of AIJ), No. 556, 25-34 (in Japanese with English abstract).

Satoh, T. (2016). "Source, path and site effects of the 2016 Kumamoto earthquake, the foreshocks and aftershocks using the spectral inversion method," *Japan Geoscience Union Meeting 2016*, MIS34-P71.

Somerville, P. G., Irikura, K., Graves, R., Sawada, S., Wald, D., Abrahamson, N., Iwasaki, Y., Kagawa, T., Smith, N. and Kowada, A. (1999). "Characterizing crustal earthquake slip models for the prediction of strong ground motion," *Seismological Research Letters*, 70(1), 59-80.

Ueshiba, H., Miura, Y., Miyahara, B., Nakai, H., Honda, M., Kakiage, Y. and Yamashita, T. (2016). "Crustal deformation of the 2016 Kumamoto earthquake detected by ALOS-2 InSAR images," *Journal of the Geospatial Information Authority of Japan*, 128, 139–146.